Proceedings of the Institution of Mechanical Engineers, Part E:
Journal of Process Mechanical Engineering. Vol 216, No. 2, 2002, pp 73-88.

MONITORING THE LUBRICANT CONDITION IN A LOW-SPEED ROLLING ELEMENT BEARING USING HIGH FREQUENCY STRESS WAVES

N. Jamaludin[1], B.Sc, MSc, D. Mba[2], B.Eng, PhD and R.H. Bannister[2], B.Sc, MSc, PhD.

[1]Dept of Mechanical and Material Engineering, UKM, 43600 Bangi, Selangor, Malaysia.
[2]School of Mechanical Engineering, Cranfield University, Cranfield, Beds. UK. MK43 0AL.

Synopsis- This paper presents the results of an investigation into the development of a reliable, non-intrusive and effective technique capable of accessing the lubrication condition within a low-speed rotating bearing. This unique monitoring system is known as pulse injection technique (PIT) and involves transmitting a Dirac pulse through a bearing via a stress waves (SW) sensor. Analysis of measured stress wave signatures differentiated between a properly and poorly lubricated bearing. This method was found to be effective as stress wave propagation is sensitive to the transmission path, which in turn is affected significantly by the type and amount of grease present in the vicinity of the working elements of a bearing.

The ability of this technique to monitor the lubrication condition within a bearing whilst in operation could be utilised to determine the appropriate time for grease replenishment or addition.

Key words- Auto-regressive coefficients, low-speed rotating machinery, pulse injection technique, RMS, rotating biological contactor, stress waves.

1.0 Introduction

The service life of bearings used on large equipment operating at low rotational speeds (< 2 rpm) are severely affected by insufficient lubrication that separates the rotating elements from the stationary raceways. This is due to the combined effect of low speed and heavy loads that generate insufficient centrifugal force to churn the grease between the rollers and the raceways. In addition, high pressures between the rolling elements and stationary raceway force grease out from the working surfaces. As a result of this phenomena, the service life of the bearing is severely reduced.

Also, lubrication properties of grease deteriorate with time as a result of mechanical working and ageing. In addition, all lubricants become contaminated in service and must therefore be replenished or changed from time to time. For very low-rotational speed bearings it is advisable to completely fill the bearing housing with grease in order to ensure that the bearing components are properly and adequately lubricated, and to protect against corrosion [1]. For all the above reasons, accessing the quality and quantity of lubricant within the bearing housing is vital in ensuring prolonged service life.

The aim of this research was to develop a suitable non-intrusive technique to determine firstly, whether sufficient grease is present in a low-speed rotating bearing. Secondly, to ascertain if the appropriate grade of grease is being employed. Both of these aims were achieved by measuring the transmissibility of stress wave (SW) signatures across the working surfaces and elements of the bearing. This involved exciting the target bearing with a Dirac pulse via a stress wave transducer, and extracting features from the response signature captured by a second SW transducer. Several researchers [2,3,4,5,6] have used a similar technique, the acousto-ultrasonic technique, to evaluate material characteristics

and to identify defects in a material. This technique has been slightly modified for this research in order to study the transmissibility of stress waves across interfaces in low speed bearings.

Acoustic emissions and stress waves are normally defined as the elastic waves generated by the release of energy from defects within the microstructure of a material. The authors considered the above definition to be suitable for application in non-destructive testing and would like to define stress waves as the transient elastic waves generated by the interaction of two surfaces that are in relative movement to each other. This definition is more suitable for the application of stress waves in the area of machine condition monitoring. The frequencies associated with the stress wave activity are above the human hearing threshold and cover a broad frequency range of between 20KHz to several mega-Hertz. In application to rolling element bearings, the interaction of surface asperities at the working face of bearing components, and, interaction between defects and mating surfaces will result in the generation of stress waves. Therefore, the ability to detect stress waves can be utilised as an effective monitoring technique, not only for defect detection, but as this paper reports, for determining the lubricating condition in a low-speed rolling element bearing.

The water industry extensively employs low-speed bearings, particularly on Rotating Biological Contactors (RBC) used for sewage treatment [7,8]. The RBC usually operates with an extremely low rotating speed of between 0.6 RPM and 1.2 RPM. This research originated due to severe bearing failures on RBC's and the system developed was to be applied on operational units.

2.0 Lubrication mechanism in a low-speed rolling element bearings

2.1 Calculation of film thickness of a low-speed bearing based on the Elastro-hyrodyamnic lubrication (EHL) approach

The lubricant condition within a bearing can be described by the lubricant specific film thickness λ, which is a measure of the degree of separation between rolling elements and raceways. When λ is less than 3 to 4, incidental metal to metal contact occurs and this leads to a reduced bearing life. Bearing wear and friction are also related to the lubricant specific film thickness [9]. ESDU [10] recommends that rolling bearings should operate with λ values of around 1, which is sufficient to ensure that the required basic rating life is achievable. Two empirical equations for calculating the lubricant film thickness are presented in this work, ESDU [10] and Hamrock and Jacobson [11]. An approximate formula developed by ESDU [10] for calculating the film thickness, h, which is dependent on load, modulus of elasticity and viscosity variation due to pressure, is given by:

$$h=2.65\ \frac{(\eta_0^{0.7} u^{0.7} \alpha^{0.54} R^{0.43})}{(E')^{0.03} W_s^{0.13}} \qquad (1)$$

whereas Hamrock and Jacobson [11] concluded that

$$\frac{h}{R} = 3.07\ U^{0.71} G^{0.57} W^{-0.11} \qquad (2)$$

where

U = dimensionless speed parameter, $\frac{\eta u}{E' R}$

G = dimensionless materials parameter, $\alpha E'$

W = dimensionless load parameter, $\frac{W_s}{E'R}$

h = minimum lubricant film thickness

W_s = load applied per unit width of contact

u = lubricant entraining velocity

R = effective radius of curvature

E' = effective modulus of elasticity

η_o = lubricant dynamic viscosity at atmospheric pressure and at operating temperature.

η = dynamic viscosity

α = pressure exponent of lubricant viscosity

Solving for the film thickness, h, yields [11]:

$$h=3.07\ \frac{(\eta^{0.71}u^{0.71}\alpha^{0.57}R^{0.4})}{(E')^{0.03}W_s^{0.11}} \qquad (3)$$

A detailed description of the determination of parameters W_s u, R and E' is given in ESDU [10]. The degree of surface asperity contact can be expressed by the ratio of the minimum thickness, h, to the combined roughness R_{qt}, known as the specific film thickness or lambda ratio, λ, where

$$\lambda=\frac{h}{R_{qt}}$$

Values for the combined surface roughness, R_{qt}, of typical rolling bearing finishes can also be obtained from ESDU [10].

The technical specifications of the test bearing used for the calculation of the film thickness is shown in table 1. Two types of grease were employed for calculations, grease

types A and B. Properties are detailed in table 2. Grease A is a general application grease while grease B is formulated specifically for slow rotating machinery.

Table 1: The test bearing, split cooper, technical specifications

Bearing type:	**Split Cooper bearing Series 01B65 EX**
Internal diameter, d:	65 mm
External diameter, D:	114.30 mm
Static load rating, L_S	110 kN
Length of the roller, l:	19.05 mm
Diameter of the roller, rd:	14.287 mm
Number of roller, Z:	12

Table 2: Properties of the lubricants used in the study

Lubricant	**Kinematic viscosity, mm^2/s at 40^oC**	**Pressure exponent of viscosity, 10^{-9} m^2/N**	**Density, kg/m^3**
Grease A	180	25 (16)	880 (16)
Grease B	1000	25 (16)	880 (16)
Oil	77.1	-	-

The properties of the lubricants shown in Table 2 together with equations 1, 2 and 3 were used to determine the film and specific film thickness for each lubricant. These

calculations were applied for a fixed load of 59.20 KN, which is slightly higher than the designed load of the test bearing, 55.00 KN. The results are presented in table 3 which shows that the calculated film thickness is in the range of nano-meters, confirming that a low-speed rolling element bearing is lubricated by a thin film. The tables also show that grease type B provides a much thicker film than type A. This is due to the fact that grease type B has a higher kinematic viscosity. These calculations show that the film thickness for a very low-speed rolling element bearing is dependent on the viscosity of the lubricant employed.

Table 3 shows that the values of specific film thickness, λ, are much lower than the recommended value of 1 [10, 11], suggesting that metal-to-metal contact would be experienced at low rotational speeds.

Table 3: Results of the film and specific film thickness calculation for all the lubricant

Lubricant	Film thickness x 10^{-9} m		Specific film thickness λ	
	ESDU (16)	Hamrock and Jacobson (17)	ESDU (16)	Hamrock and Jacobson (17)
Grease A	8.8320	8.5773	0.0245	0.0238
Grease B	29.3335	28.9806	0.0815	0.0805

2.2 Thin Film Lubrication

Since the calculated film thickness for the test bearing is in the range of nano-meters, the lubrication regime between the rolling elements and the raceways of the low-speed

bearing can be classified as thin film lubrication (TFL). Several researchers [12,13,14,15,16,17,18] have studied the thin film lubrication mechanism. Jang and Tichy [16] define the thin film lubrication regime as that in which the film thickness is of the same order as the molecular scale of the lubricant, that is in the region of nano-meters. The lubricant molecular scale is approximately in the region of 1 nano-meter compared to the roughness height of high quality bearing or gear surfaces, approximately 25 nano-meters. These observations suggest that bearings at low rotational speeds will be prone to early loss of mechanical integrity.

3.0 Experimental Technique, Procedure and Apparatus

The propagation of surface waves at interfaces is similar to pressure waves transmitted across two surfaces in contact. However, as the surface asperities are quite rough, only part of the surface area is actually in contact. As stress is a force per unit area, the actual area transmitting force is very small. If the microscopic gaps between asperity contact points are filled with a liquid, the pressure will be uniformly transferred between the surfaces. Since the propagation of stress waves across interfaces is dependent on the transmissibility of the couplant/liquid and amount of surface contact, this phenomenon can be utilised as a tool to monitor and identify the presence of a lubricant between working faces of a low-speed rolling element bearing. If stress waves are forced to propagate through these interfaces, and the resultant energy of the stress waves measured, these results could be related to the lubrication condition in the bearing. It is expected that a properly lubricated bearing element will transmit more energy of a SW compared to a poorly lubricated bearing, as there would be more contact between asperity points and the lubricant.

A preliminary study was undertaken on the propagation characteristics of stress waves across interfaces. The study involved transmitting a stress wave across two steel blocks with differing lubricants between the blocks. A further test was also undertaken where a steel beam replaced one of the blocks detailed above. This second test was undertaken firstly, for authentication, but also to assess the effects of a long transmission path on the SW for different lubricant types. The results of this initial study were applied in assessing the lubricating condition of a low-speed rolling element test bearing.

3.1 Preliminary tests of stress wave propagation across an interface

The purpose of the preliminary tests was to study the transmissibility characteristic possessed by oil and types A and B grease, through an interface. Type A grease is a general application grease whilst type B grease is formulated specifically for slow-speed rotating machinery. Weighing the grease and oil for all tests ensured repeatability.

3.1.1 Stress wave propagation through two test blocks

A schematic diagram of the test blocks arrangement is shown in figure 1 (a) and a photograph in figure 1 (b). The size of each steel block was 50mm (length) x 40mm (width) x 25mm (thickness). Three types of lubricant were used in this study and all their properties have been detailed in table 2. For each test, 0.75 grams of a lubricant was spread evenly on one of the tests blocks. The lubricant was weighed using PAG Oerlikon weighing equipment type 250-9320 capable of weighing between 0.000g and 500.000g.

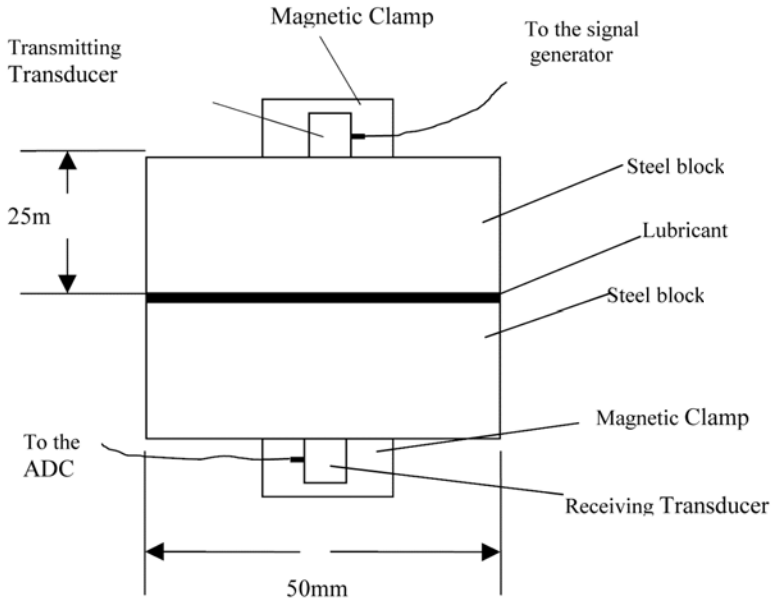

Figure 1 (a): Schematic diagram of the test blocks arrangement for the PIT technique.

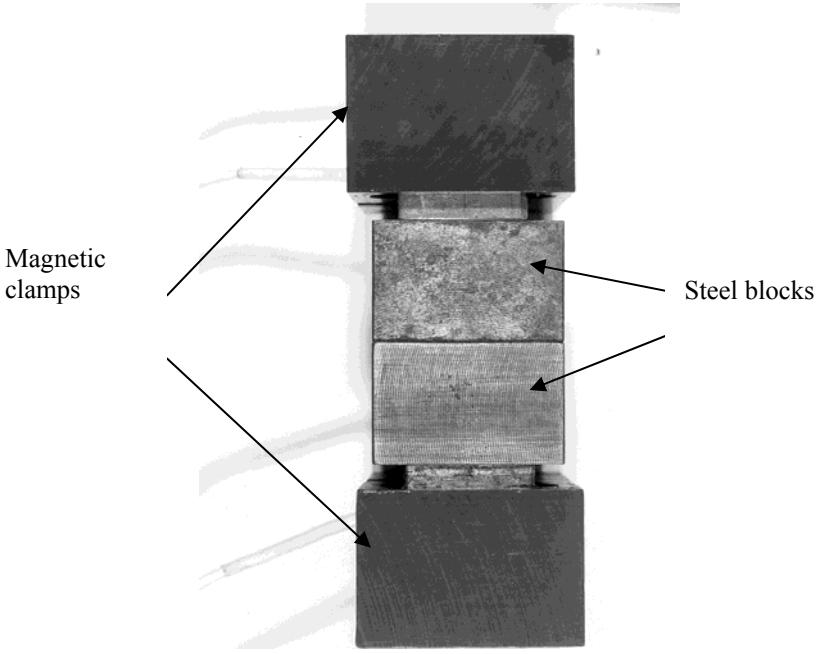

Figure 1 (b): End view of test blocks arrangement for the PIT technique.

The data acquisition system consisted of a Physical Acoustic Corporation (PAC) broad band AE transducer, model number WD/AD35. Amplification was provided with the use of a PAC pre-amplifier type 1220A and a post-amplifier, type AE1A. A dual channel

Analogue-to-Digital (ADC) converter from Rapid Systems (type R2000) was used for data acquisition whilst and a Hewlett Packard model 8111A signal generator was employed to generate a Dirac pulse.

The transducers were attached to the steel blocks using a magnetic clamp to obtain uniform force throughout the tests. The type B grease was used as the couplant for both the transmitting and receiving transducer. Both transducers and magnetic clamps were left undisturbed throughout the tests. Finally, the signal generator was used to input a Dirac pulse with an amplitude of 5.0 volts and a bandwidth of 100 nano-seconds via one of the transducers. The resultant signature was captured at a sampling rate of 20MHz.

3.1.2 Stress wave propagation through a long steel beam

A schematic diagram of the beam-block test arrangement is shown in figure 2 (a) and a photograph in figure 2 (b). The size of the steel beam was 1200mm (length) x 30mm (width) x 15mm (thick). Again, the transducer was attached to the top of the steel beam using a magnetic clamp in order to maintain a consistent clamp force throughout the tests. The magnetic clamps and the transducers were left undisturbed throughout the tests. A Dirac pulse with an amplitude of 8.0 volts and a bandwidth of 100 nano-seconds was used to excite the steel beam via a SW transducer.

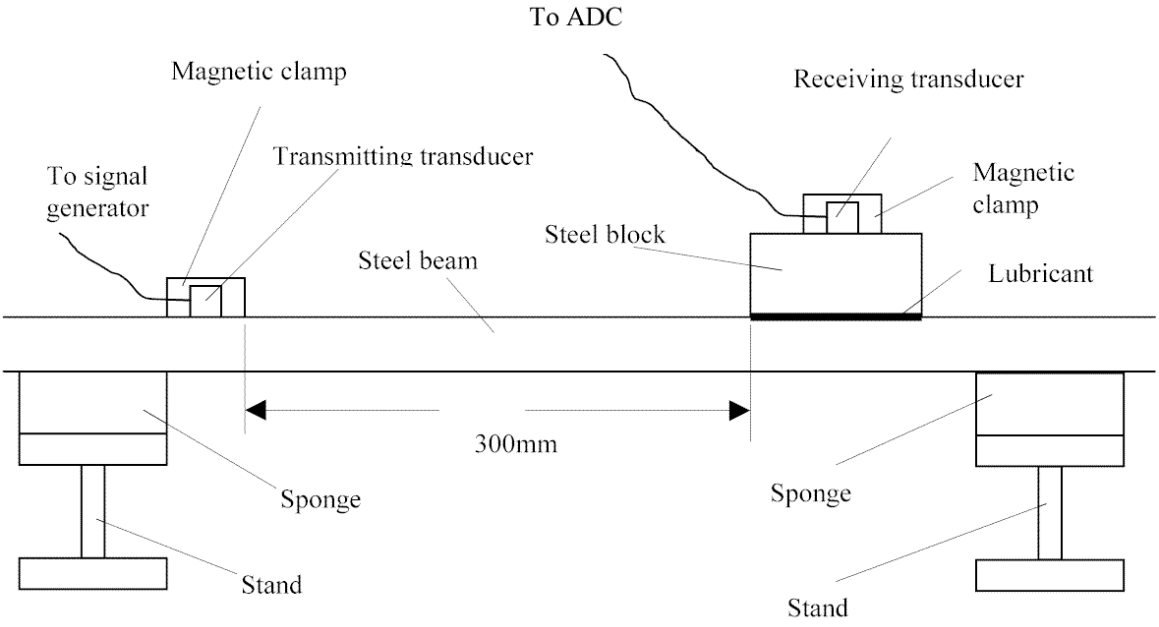

Figure 2 (a): Schematic diagram of the steel block and beam arrangement for PIT technique.

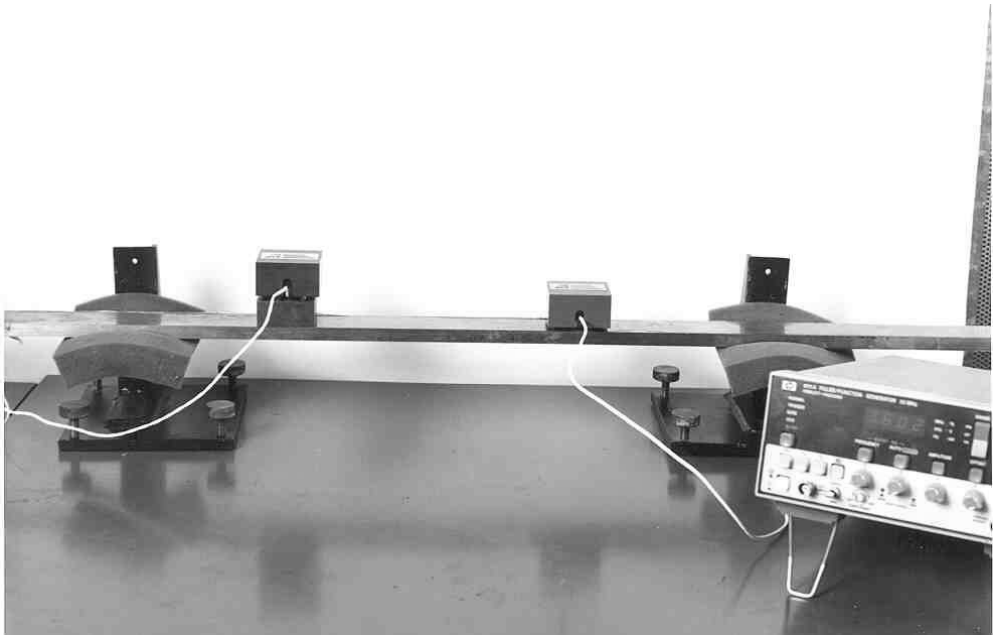

Figure 2 (b): Picture of the steel block and beam arrangement for PIT technique

3.2 Application of stress wave propagation test on the test-rig

3.2.1 Test-rig

A photograph of the test rig is shown in figure 3 (a) and a schematic in figure 3 (b). The main components of the test rig consist of a motor/gearbox system, two support bearings acting as slave bearings, the test bearing and hydraulic cylinder ram. The test bearing was a spherical roller bearing selected from a split Cooper bearing. This type of bearing was selected as it is commonly used on RBC's. The test rig was driven by an electric motor via a gear box system The motor/gear box system was a KA96R62 Helical-Bevel geared motor, providing a rotational speed of 1.12rev/min. Load was applied to the test bearing via a hydraulic cylinder ram supported by a 'H' frame. Identical loads were applied on all tests.

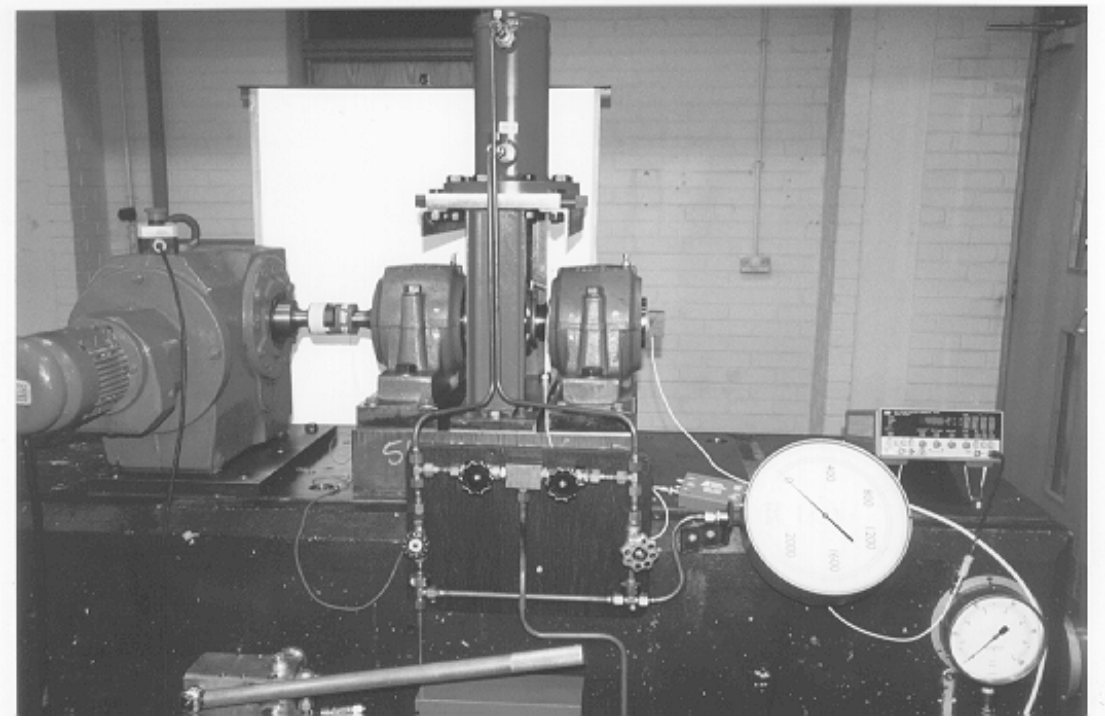

Figure 3 (a) Photograph of the test-rig

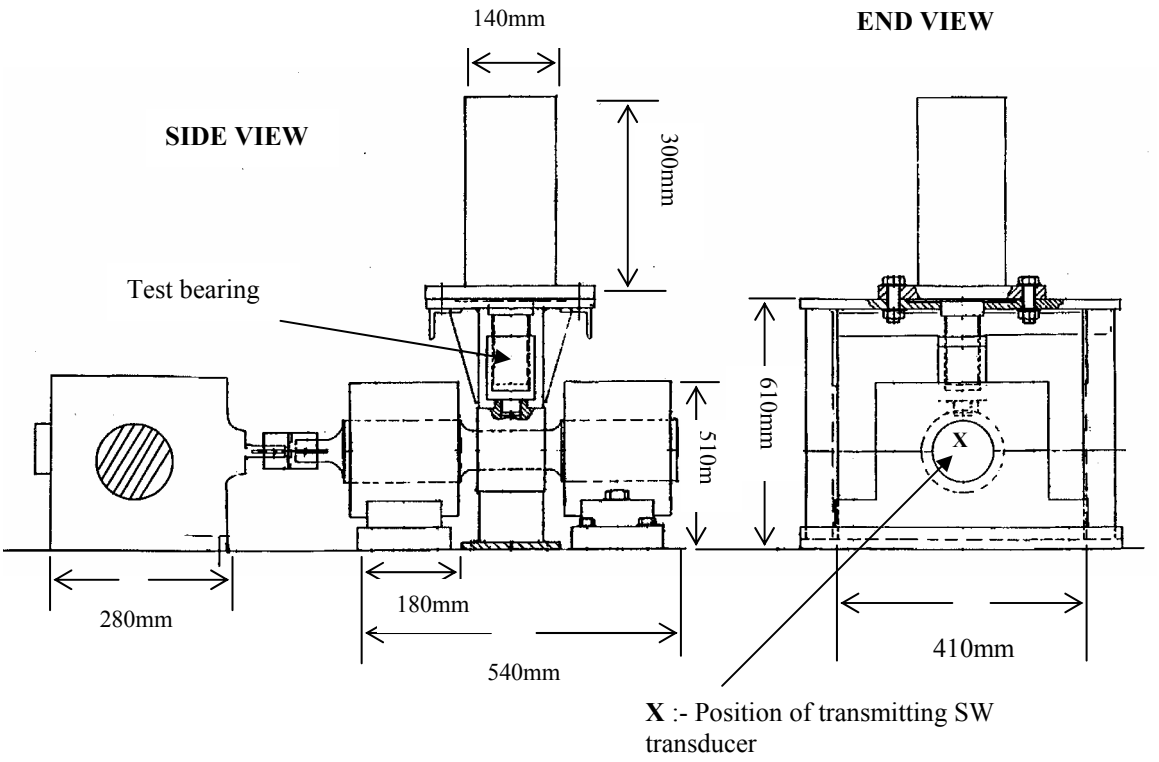

Figure 3 (b) Schematic diagram of the test-rig

3.2.2 Pulse injection technique (PIT)

The pulse injection technique (PIT) was conducted on the test-rig by transmitting a Dirac pulse via a stress wave transducer attached at the centre of the shaft as shown in figures 3(a) and 3(b). The pulse was transmitted while the shaft was rotating and measurements were obtained for several rotations of the shaft. The pulse was transmitted at regular intervals/positions during one complete revolution, namely a quarter turn (90°), one half (180°), three quarter (270°) and full (360°) rotation of the shaft. To avoid recording any background noise originating from inside the bearing, the acquisition system was put on 'hold' in-between pulse transmissions. The response of the test bearing due to the pulse was captured using a second stress wave transducer attached on the test bearing housing.

The authors believe that this technique has not been used before to study the condition of lubricant inside a bearing.

Various grease filling/capacity conditions were simulated for these tests. This involved filling the test bearing with the grease up to 'full', 'half full', a 'quarter full' and 'one-eight full' capacity. Weighing the grease identified the filling capacity of the test bearing. The application of oil was achieved by manually spreading oil onto the bearing components.

A Dirac pulse of 100 nano-sec bandwidth and amplitude of 16.5 volts was transmitted to the test bearing. This type of pulse was selected as its frequency response is flat over the frequency range of the stress wave sensors employed (100KHz to 1.2MHz). A pulse was transmitted to the test bearing for each grease type and grease capacity, in order to study the effect of the amount and type of grease inside the test bearing on the resultant stress wave signature. Before exciting the test bearing, it was allowed to rotate for about 15 minutes, ensuring an even distribution of lubricant within the bearing.

4.0 Experimental Results and Discussion

4.1 Signal Processing Technique

The recorded signatures had to be classified so as to identify the type of grease employed and the amount of grease inside the bearing. The process of feature extraction involved simple time series features for observing changes in signature strength, RMS, peak amplitude and energy.

It was thought prudent to establish a more robust technique for classifying and grouping signatures based on the effects of the transmission paths. The philosophy behind this was that the interpretation of parameters such as amplitude, RMS and energy of SW signatures from operational bearings might not necessarily indicate the condition of the lubricant within the bearing. This could be the case where levels of background noise, which will vary from one bearing to another, could mask out SW signatures produced by the PIT; therefore, determination of lubricant condition would be impossible. Mba et. al. [7,8] have shown that transmission paths can aid in source location of SW signatures by classification of Auto-Regressive (AR) coefficients associated with each SW. As it is anticipated that the effect of the lubricant transmissibility will affect the transmission characteristics, and thus signature shape, the technique of classification based on an AR model was undertaken.

Oksa [19] and Mba et.al. [7] showed that the shape of a burst can be represented by a few Auto-Regressive (AR) coefficients. Auto-Regressive modeling has been detailed by Kay et al [20] and Makhoul [21] and the computation of AR coefficients is derived from linear prediction [22]. To aid fault/source identification, a clustering process that grouped the AR coefficients associated with each SW signature was employed. This is a hierarchical technique that measures the Euclidean distances between the centroid value of the AR coefficients associated with each signature. Initially the coefficients with the minimum distance are grouped together. Next, the group's centroid position is recalculated, and the AR coefficients with the minimum distance to the newly formed group are clustered with it. This procedure is repeated every-time a component is added to the cluster until all the components are grouped. The results of classification were represented graphically using

an agglomerate dendrogram plot [23] in which individual signals are labelled on the y-axis whilst the distance between the centroids of clusters are shown on the x-axis.

4.2 Results :- PIT for the steel blocks

Typical stress wave signatures transmitted across the steel blocks when lubricated by grease types A, B, oil and under dry condition are shown in figures 4 (a) to 4 (d) respectively. The figures show two signatures for each lubricant condition, indicating clearly the repeatability and consistency of the acquired results.

Amplitude, RMS and energy features were extracted for each signature and the results are detailed in table 4. Clearly, type B grease provided the best transmissibility across interfaces for the input stress waves. Based on the acquired results, it is evident that the higher the lubricant viscosity, the stronger the resultant stress waves signal that can be transmitted across an interface.

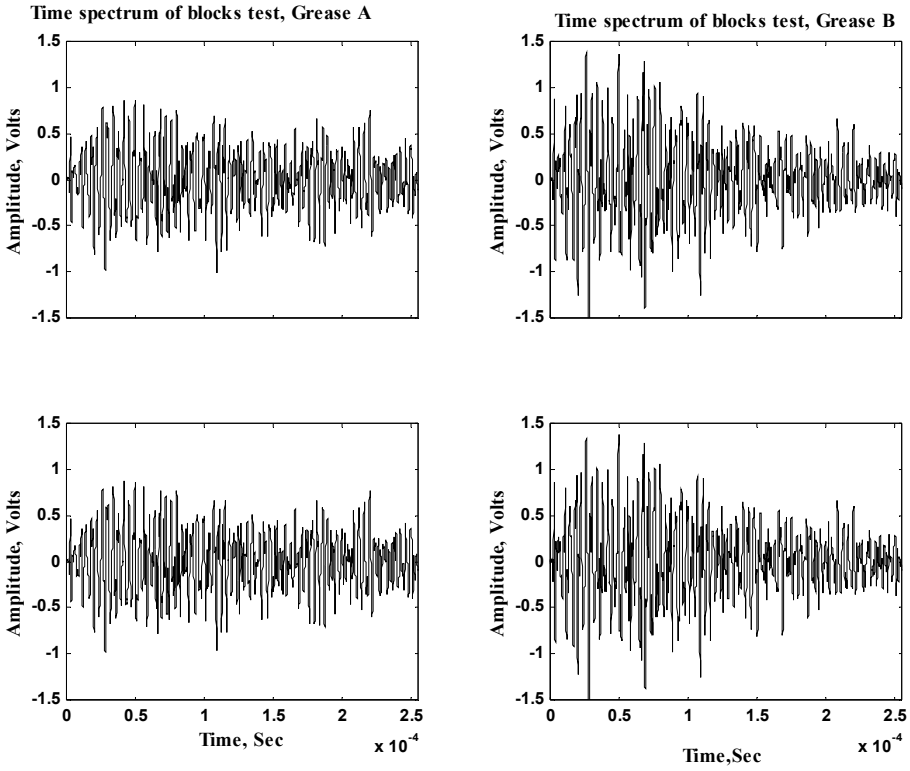

Figure 4 (a-b): Typical stress waves signatures for steel block tests

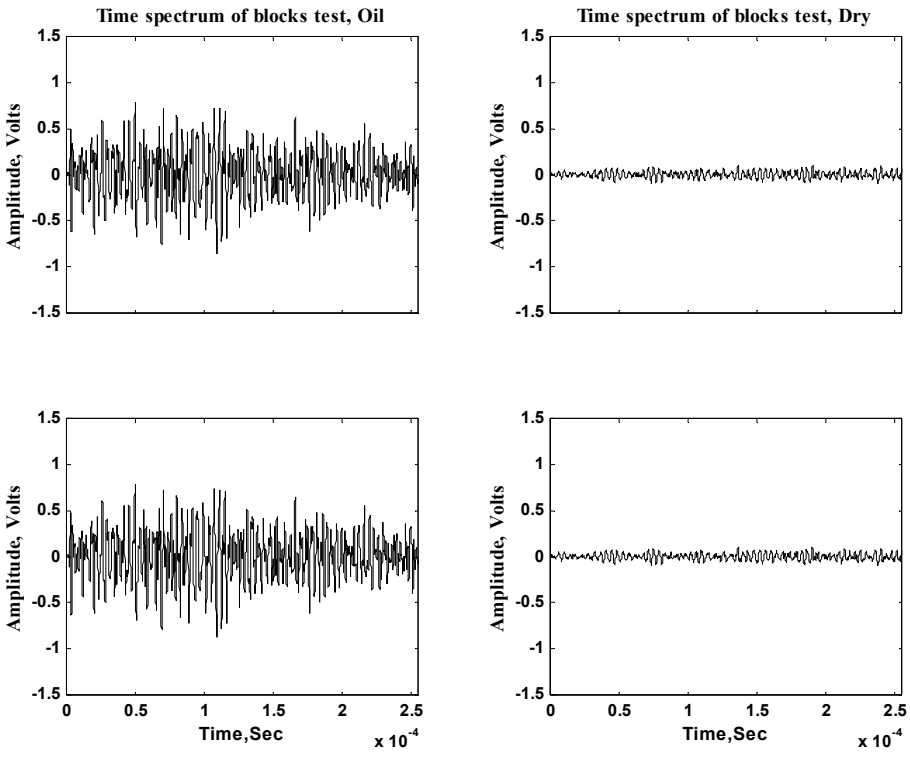

Figure 4 (c-d): Typical stress waves signatures for steel block tests

Table 4: Averaged values of amplitude and energy for different lubricant used in PIT for the steel blocks

Lubricant	Amplitude, rms (Volts)	Amplitude, max (Volts)	Energy (Volts.msec) x 10^{-6}
Dry	0.0357	0.1012	0.9474
Oil	0.2564	0.7700	24.6956
Type A grease	0.2729	0.7560	36.9112
Type B grease	0.3972	1.3920	46.463

Five signals from each type of lubricant were represented with a 10^{th} order AR model. Selection of the model order was based on Akaike's information criterion (AIC) and the forward prediction error (FPE) [20,21]. Figure 5 shows the results of the classification based on the AR coefficients associated with SW's of each grease type. Every signature associated with the lubricant condition is clearly displayed, for instance all five signatures associated with grease type A are labelled 'a1' to 'a5'. This method of numbering signatures associated with a lubricant condition is undertaken throughout this paper. The results of classification show that the signatures for the type B grease and dry condition could be identified easily from lubricant types A and oil signatures. This indicates the capability of the AR algorithm to characterise the stress wave signatures associated with differing lubricant viscosities. As lubricant type A and oil have similar viscosities in relation to type B, it explains why they were grouped together. The classification results have a similar trend with those obtained using the amplitude, RMS and energy analysis, as there is a clear distinction between type B grease and the dry condition, though type A and oil have similar results.

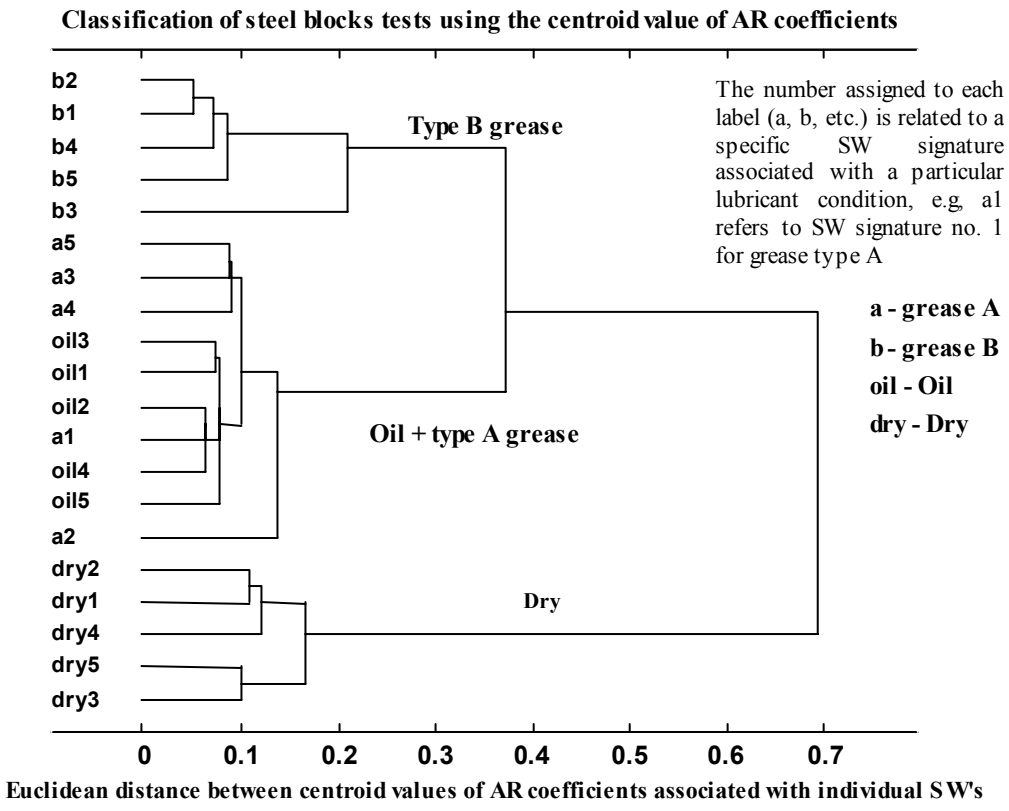

Figure 5: Classification of the PIT signatures based on the AR coefficients, steel blocks test

4.3 Results :- PIT for the steel beam

Figure 6 (a) to (d) show signatures associated with the steel beam block experiment. The results detailed in table 5 also show that type B grease provides the best transmissibility across interfaces of the beam/block. The amplitude and energy of the recorded signature of type B grease is approximately four times higher than that of type A grease and oil. This is in agreement with our previous test.

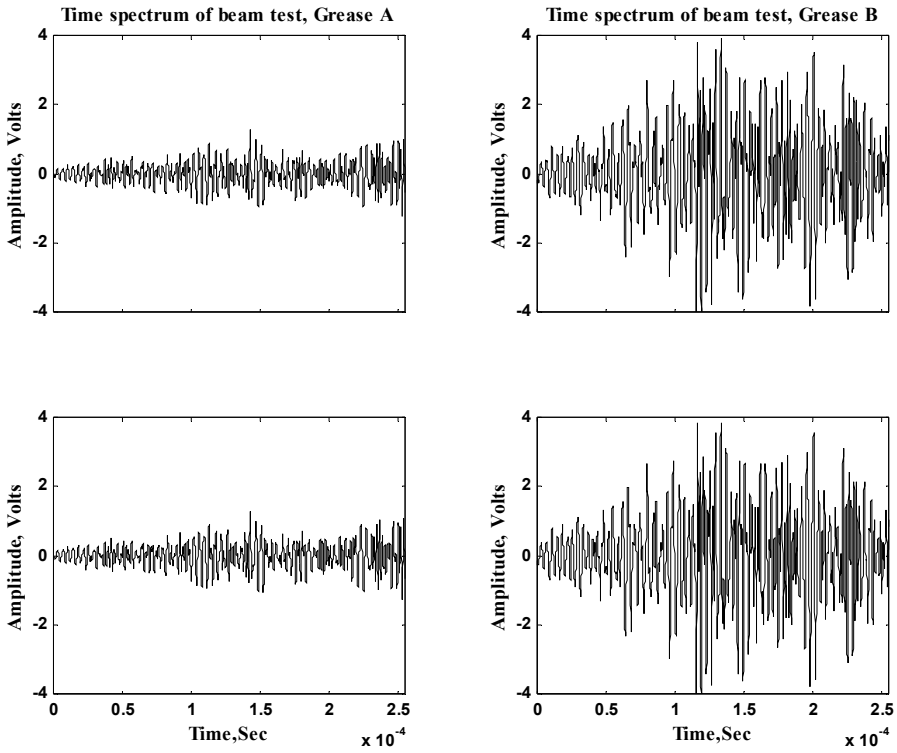

Figure 6 (a – b): Typical stress waves signatures for steel beam tests

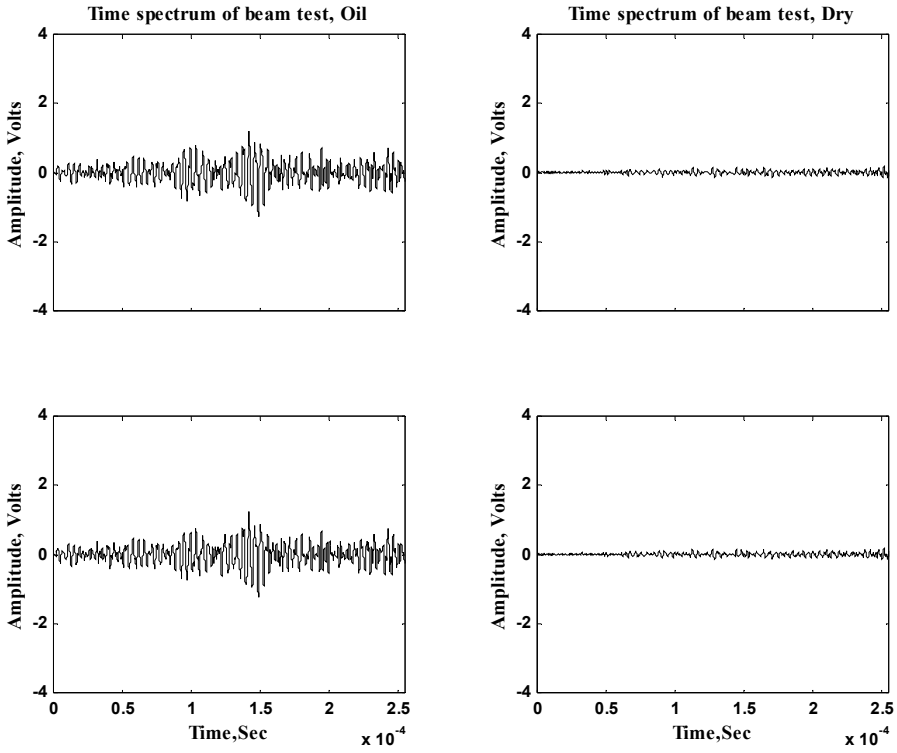

Figure 6 (c – d): Typical stress waves signatures for steel beam tests

Table 5: Averaged values of amplitude and energy for different lubricant used in PIT for the steel beam test

Lubricant	Amplitude, rms (Volts)	Amplitude, max (Volts)	Energy (Volts.msec) x 10^{-6}
Dry	0.0467	0.1572	2.7613
Oil	0.2864	1.1880	59.0536
Type A grease	0.3294	1.2680	90.5327
Type B grease	1.2630	3.9100	714.4456

Figure 7 shows the results of the classification using the AR coefficients (10^{th} order model) associated with each signature. Grouping of each lubricant is distinct and clearly visible, though lubricants type A and oil are still closely related, evident by their close grouping in figure 7. The reason for the clearer distinction between lubricants type A and oil is attributed to the longer transmission paths to the receiving sensor, allowing more pronounced effects of the lubricant viscosity on the stress wave signature. These changes in signature shape will result in distinct groups based on clustering associated AR coefficients.

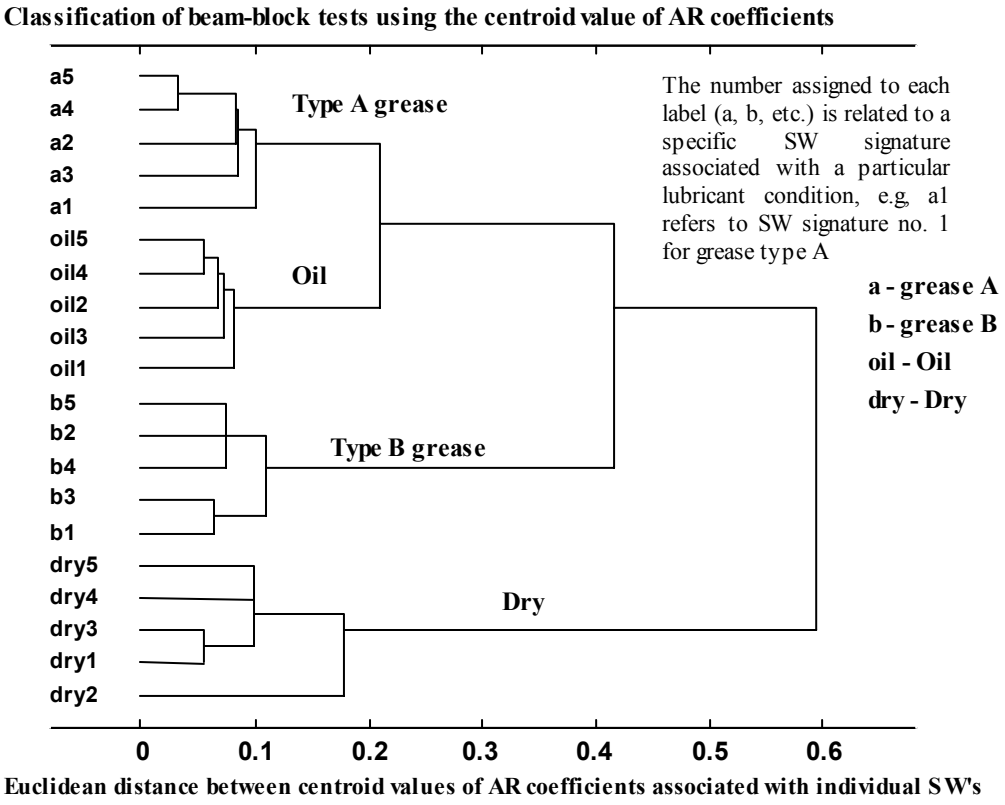

Figure 7: Classification of the PIT signatures based on the AR coefficients, steel blocks test

The results for both steel blocks and beam tests show conclusively that the transmissibility of stress waves across interfaces is affected by the lubricant viscosity and transmission path.

4.4 Application of the pulse injection technique on the test-rig

The most direct transmission path for propagation of a stress wave across a bearing is through the interfaces between the inner race, the rolling elements and the outer race. This is particularly applicable when the rolling element is in the loading region. The

bearing lubricant will not only ensure that the loads are evenly distributed between the rolling elements and raceways, but also fill any microscopic gaps. Therefore, the propagation of a stress wave across the bearing will be sensitive to the different lubricant transmissibility characteristics as indicated by the results of the steel beam arrangement.

Figure 8 shows the resultant signatures for type B grease (capacity: - full) at shaft positions 90°, 180°, 270° and 360° of rotation. These signatures vary slightly for different positions of the shaft. This indicates that the position of the rolling elements inside the bearing housing has an effect on the transmission path of the input pulse. For instance, there might not necessarily be a roller in the load region to provide a more direct transmission path to the receiving SW transducer. In this case the transmission of the SW is dependent on the amount of lubrication within the bearing housing. For this reason it is expected that there will be a variation in shape and characteristics (energy, amplitude, RMS) of the resultant signature. This highlights another potential drawback with extracting simple time series features (energy, .. etc.) and provides an adequate test for the AR classification model.

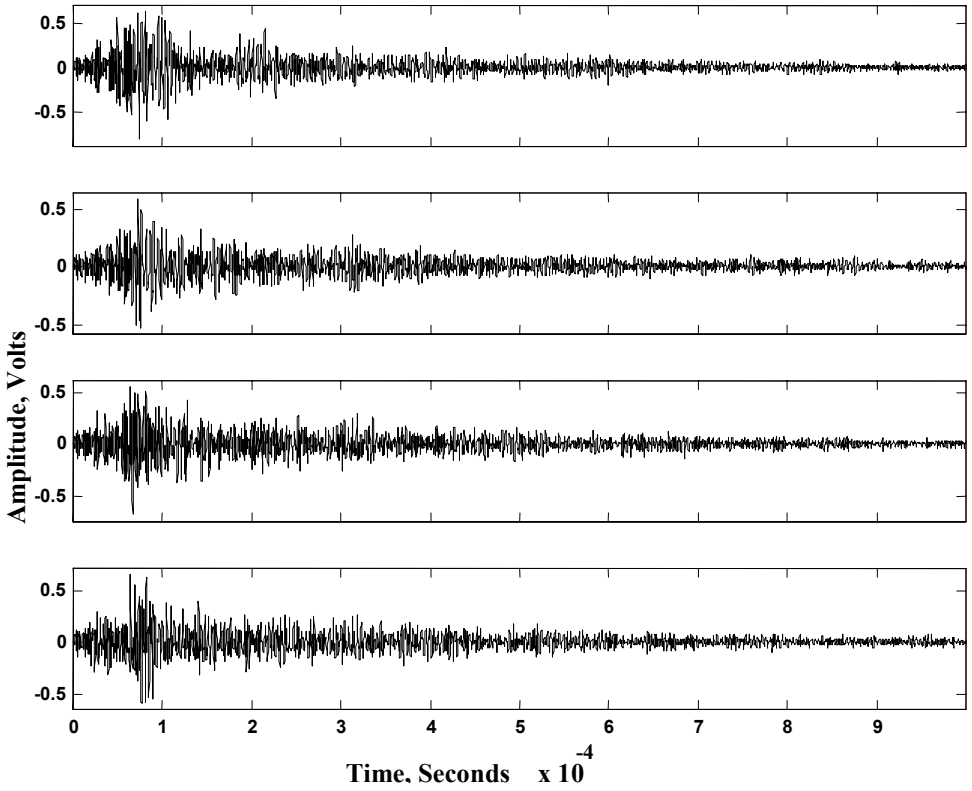

Figure 8: Resultant time waveform of the PIT for grease type B with full condition at the shaft position of 90°, 180°, 270° and 360°.

The results of the time series analysis for both dry condition and oil lubrication are shown in table 6. The sets were obtained by averaging twenty resultant signatures acquired from five revolutions of the shaft. Furthermore, the results show differences in transmissibility between the dry condition and oil lubrication, particularly in terms of energy.

Table 6: Results of the PIT signal acquired for dry condition and oil lubrication

Lubricant	Averaged Amplitude, rms (Volts)	Averaged Amplitude, max (Volts)	Energy (Volts.msec) x 10^{-6}
Dry	0.0214	0.0932	0.1235
Oil	0.0232	0.1301	0.5512

Table 7: Time series analysis of the resultant PIT signal with different amounts of grease inside the bearing

Lubricant	Amount of grease			
	Full	**1/2 Full**	**1/4 Full**	**1/8 Full**
Averaged RMS (volts)				
Type A grease	0.1148	0.0300	0.0321	0.0300
Type B grease	0.1377	0.0712	0.0300	0.0335
Averaged Peak (volts)				
Type A grease	0.4901	0.1189	0.1204	0.1010
Type B grease	0.6269	0.2670	0.1046	0.1058
Averaged Energy (Volts.msec)x10^{-6}				
Type A grease	7.3127	0.7624	0.8610	0.5820
Type B grease	8.9204	2.3598	0.6560	0.7194

Table 7 shows the results for RMS, peak amplitudes and energy for grease types A and B with varying capacities inside the bearing. These show clearly that the amplitude and energy levels decrease significantly with the amount of the type A grease inside the

bearing. Energy levels decrease by approximately 90% when the amount of the type A grease was reduced from 'full' to 'half' full. In addition, the table also shows that the amplitude and energy levels vary very slightly when the amount of the type A grease was reduced from half to one-eighth full condition. At filling capacities of a 'half', a 'quarter' and 'one-eight', the amplitude and energy levels of type A grease were only slightly higher than the oil and dry lubricating conditions. Therefore, this result may indicate that the type A grease loses most of its transmissibility when the amount of grease inside the bearing reduces to a half full.

Also, table 7 shows that the amplitude and energy levels of type B grease decrease uniformly and substantially when the capacity was reduced from 'full' to a 'quarter full' condition. For example, the energy level decreases by approximately 74% when the amount of type B grease was reduced from 'full' to 'half full' condition and from 'half full' to a 'quarter full' condition. Further reduction of the amount of grease does not significantly affect the amplitude and energy levels of the resultant signal. This may indicate that the type B grease loses most of its transmissibility when the amount of grease inside the bearing reduces to a quarter full condition.

These results demonstrate the superiority of the higher viscosity grease in providing better transmissibility across interfaces for the input stress waves at defined grease capacity levels. This is in accordance with the result obtained from the preliminary tests using steel blocks and beam, and indicates that lubricant viscosity plays a vital role in transmitting stress waves for both static and dynamic systems.

Both types A and B greases show that the averaged amplitude and energy levels can be utilised as a measurement criteria to detect the amount of grease present in a low-speed bearing. The authors suggest that the energy level should be used as an indicator, since there are significant changes in the energy level when the amount of grease in the bearing reduces from its full condition. Energy level can easily be used to alert the maintenance team regarding the amount of grease left in the bearing. Therefore, a trending technique is suggested to monitor the variation of the energy level of the resultant PIT signal over a period of time. Also, this parameter could be used to monitor the lubricant condition, i.e., deterioration in viscosity.

Figure 9 shows the results of the classification of the SW signatures associated with type A lubricant using AR coefficients. Four groups emerged after classification. The close-up views of figure 9 are provided in figures 10 and 11. SW signatures associated with the full capacity were grouped together, that is cluster 1 of figures 9 and 10. Signatures for the other capacities, one half, one-quarter and one-eighth full were grouped together in two clusters, clusters 2 and 4. However, the dry condition was clearly grouped in cluster no. 3. These classifications correlate favourably with amplitude, energy and RMS features detailed in table 7. There was a clear difference in extracted features (table 7) from a ‘full’ to ‘half’ full condition and this is mirrored in the classification results. Also, the classification was able to differentiate and group signatures associated with the dry condition. This demonstrates a clear distinction in signature shape between full, dry and other conditions. The cluster groups were determined by observing what signatures were clustered together, for instance, in figure 10, cluster 1, all signatures associated with the full condition fell into this group, see labels on y axis. The notation 'f6’ refers to SW signature number 6 for a full grease capacity (note legend on figure).

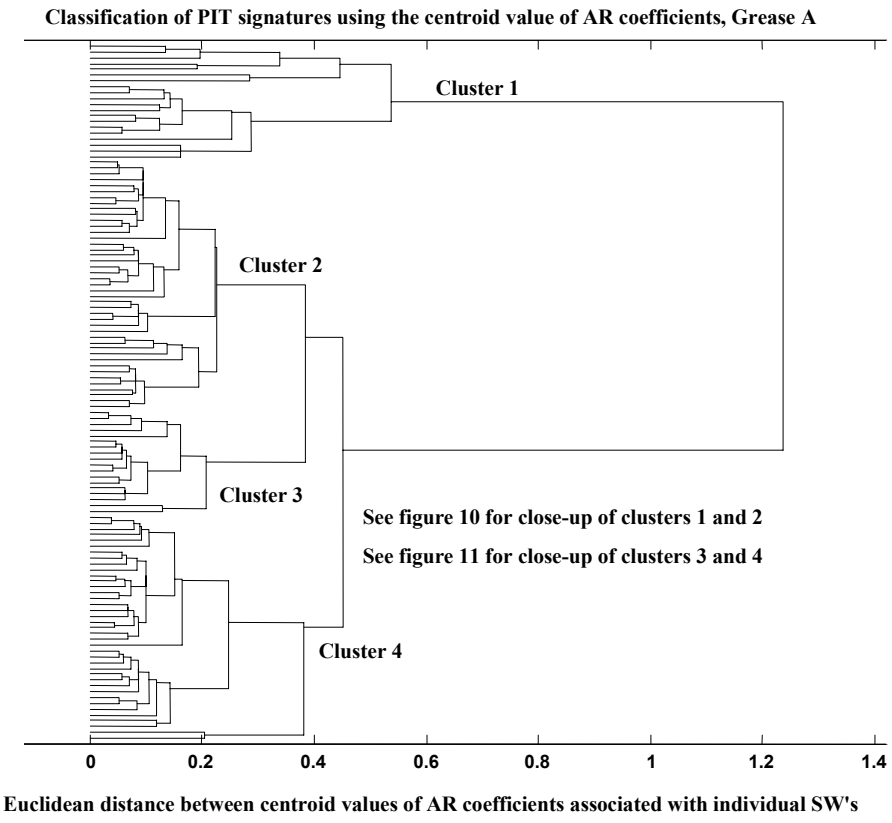

Figure 9: Classification of all filling capacity, oil lubrication and dry condition signatures based on AR technique, grease A.

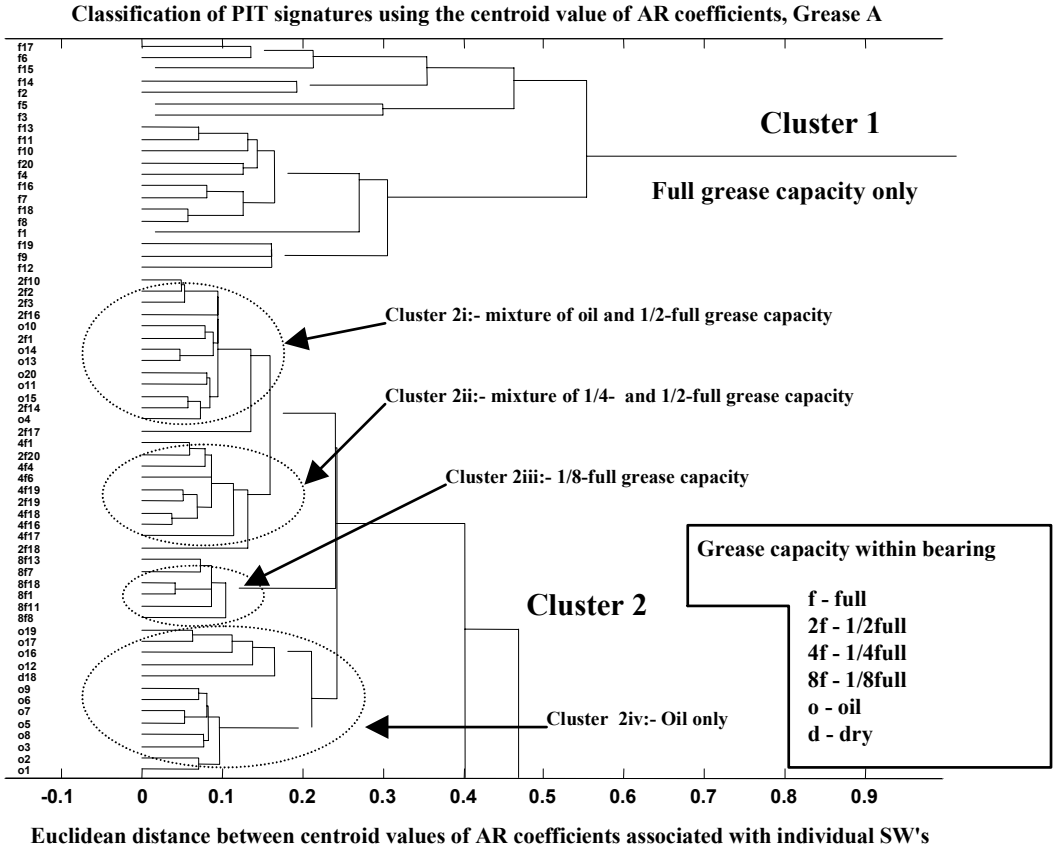

Figure 10: Close-up view of clusters 1 and 2 of figure 9.

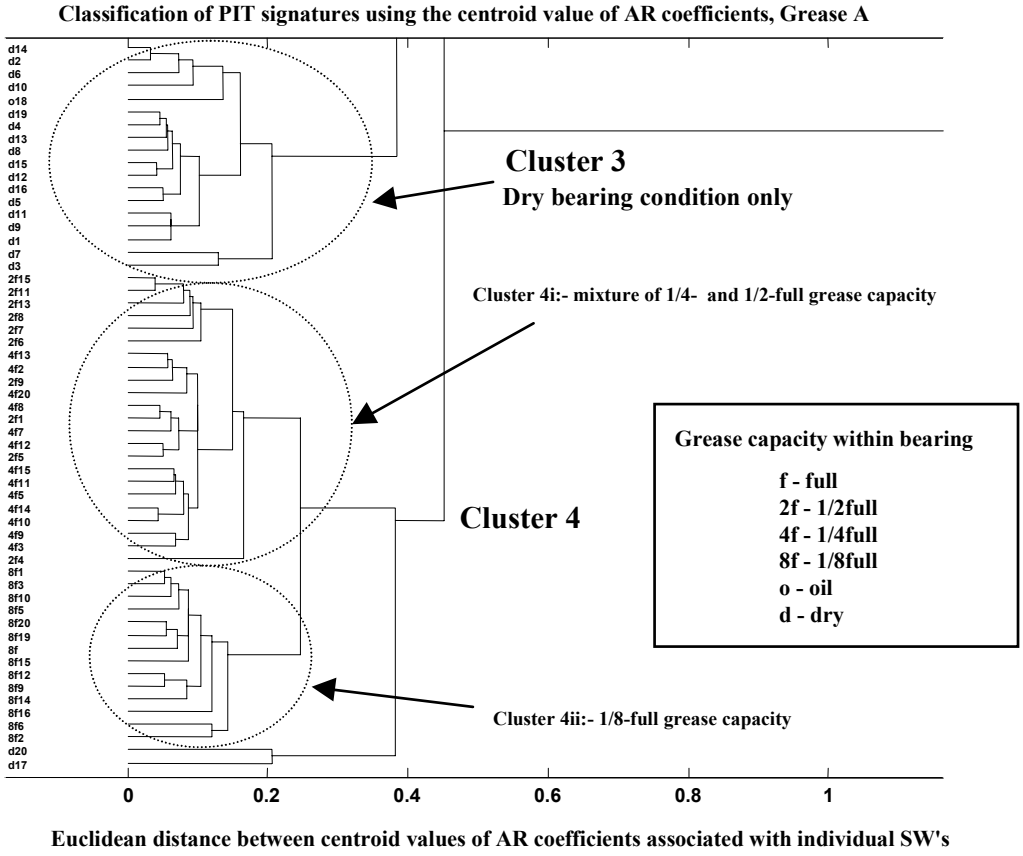

Figure 11: Close-up view of clusters 3 and 4 of figure 9.

Classification of auto-regressive coefficients associated with type B grease is shown in figure 12. The figure shows that the signals for each filling condition were clustered into three main clusters. The close-up views of figure 12 are shown in figures 13 and 14. The 'full' and 'half'-full signatures were grouped together in cluster 3 as shown in figure 14 and the rest of the groups, clusters 1 and 2, consisted of a mixture of all other conditions.

The results of classification indicate that as the condition of lubricant within the bearing deteriorates, distinct groups become evident. Type A lubricant appears to lose its SW transmissibility, and thus its lubrication effectiveness, as the capacity reduces from 'full' to 'half' full. However, type B only loses its effectiveness after the capacity has been reduced from 'half' full to a 'quarter' full. This suggests that the classification of AR

coefficients associated with SW's has the capability of recognising and differentiating the transmissibility characteristic provided by different amounts of grease.

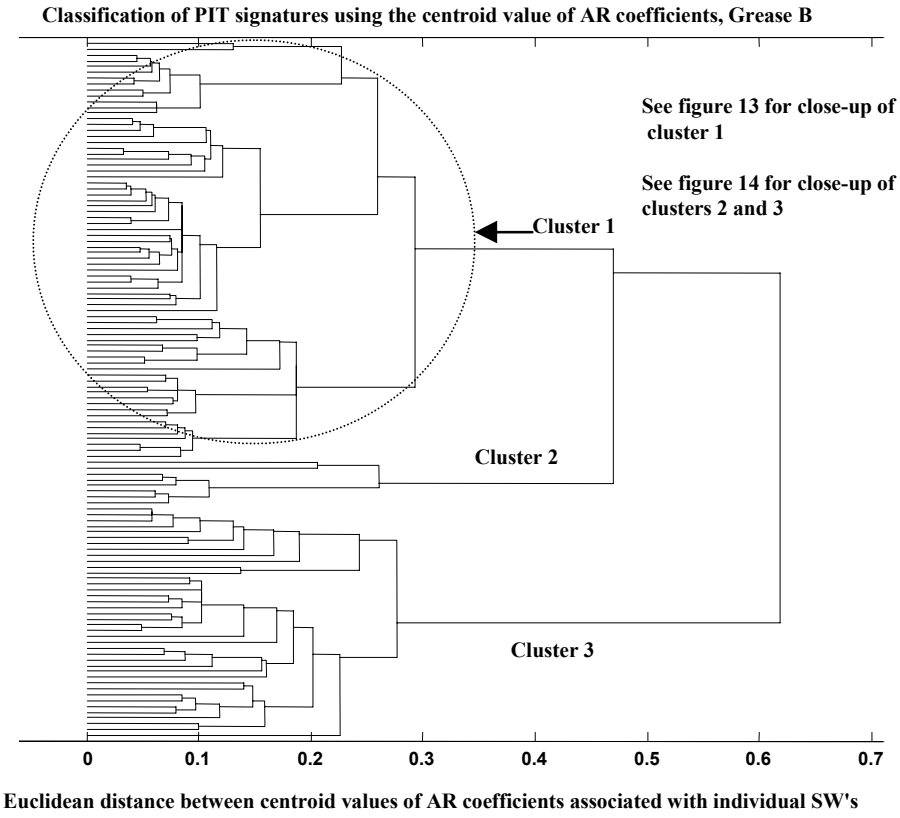

Figure 12: Classification of all filling capacity, oil lubrication and dry condition signatures based on AR technique, grease B.

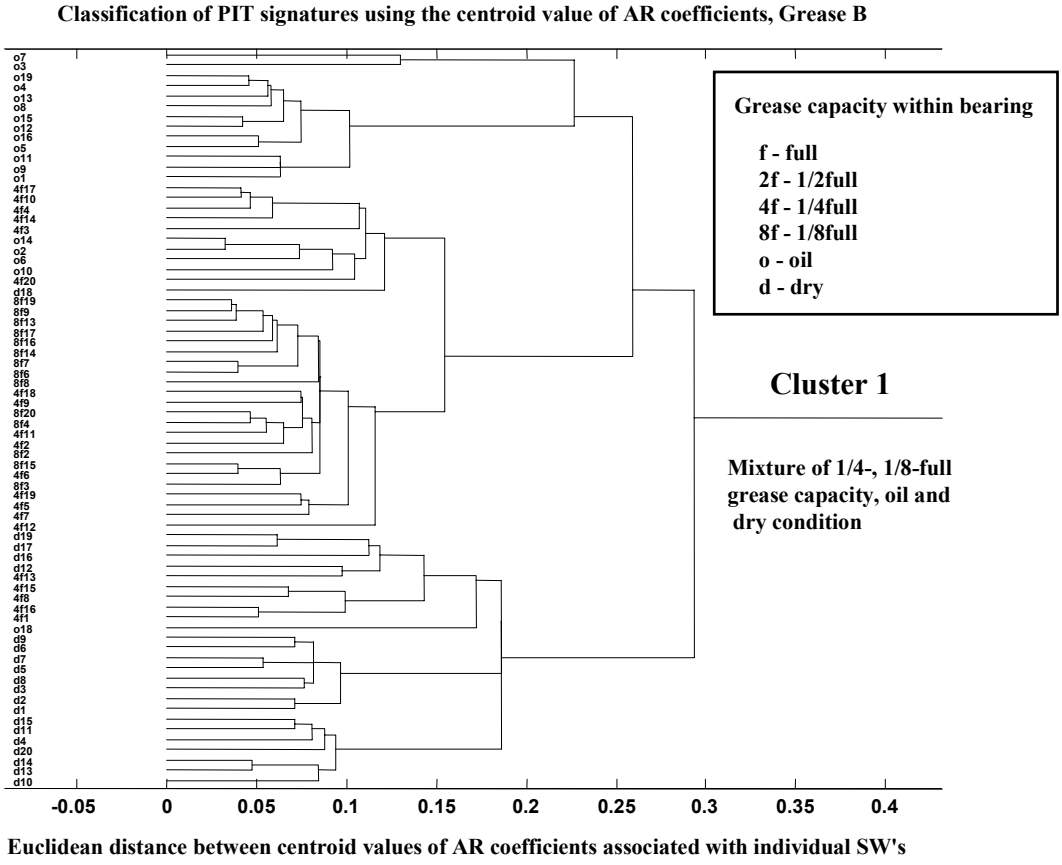

Figure 13: Close-up view of clusters 1 and 2 of figure 12.

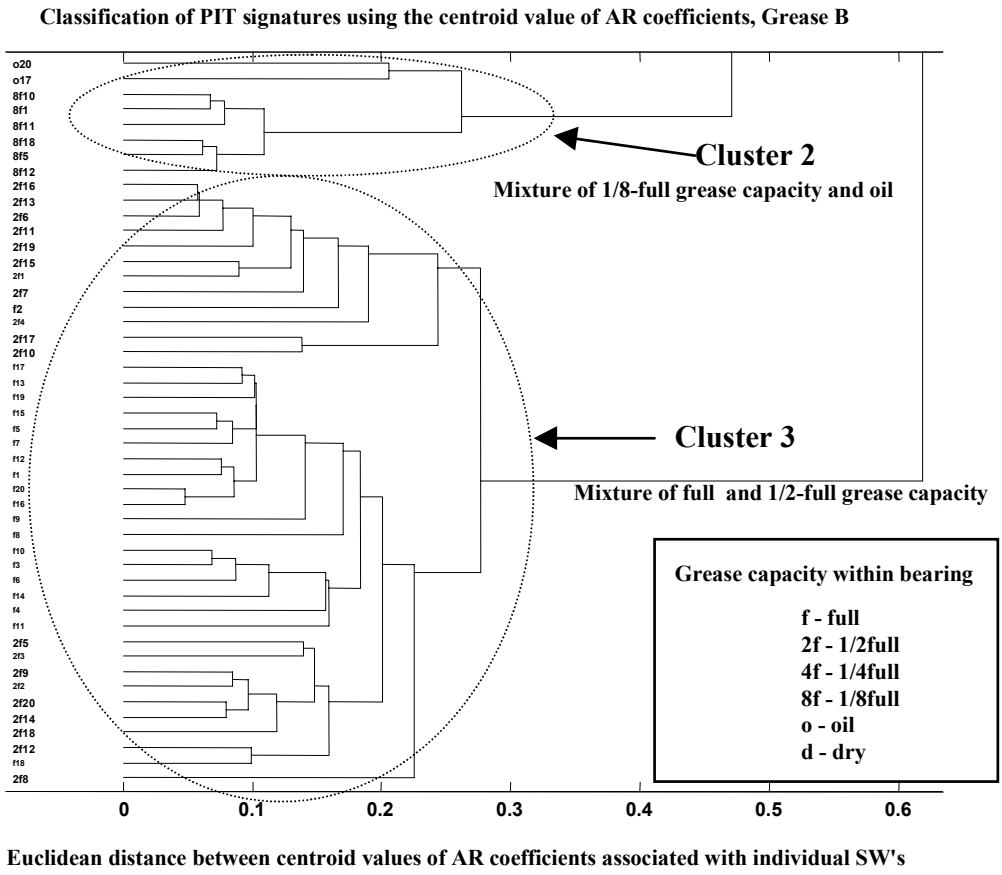

Figure 14: Close-up view of clusters 3 and 4 of figure 12.

The successful grouping with AR coefficients, which mirrored results of RMS, amplitude and energy levels, proves that this method is not affected by slight changes in signature shape that could arise from varying positions of the rolling elements during acquisition. This highlights the robustness of the method of AR feature extraction and grouping.

In order to utilise the energy analysis and AR algorithm to determine the amount of grease inside a low speed bearing, baseline signatures for a full condition with fresh grease is required as a reference signal. The baseline data will then be used to trend the energy level to identify any significant change in the amount of grease inside the bearing. In addition, the baseline signatures will also be used in the classification process using the AR coefficients.

After a period of time, the viscosity of grease will reduce due to ageing and contamination. Consequently, it is expected that the transmissibility capability of grease will also reduce accordingly. This phenomenon is detectable with the pulse injection technique since the reduction in transmissibility will result in the reduction of energy levels and changes in signature shape.

5.0 Conclusion

It has been demonstrated that the transmutability of SW across interfaces is dependent on the viscosity of the lubricant. Based on the results of this study, the pulse injection technique (PIT) has demonstrated its capability in assessing the amount of grease within a bearing housing, which is closely associated with the lubrication condition in the bearing. This method is found to be effective due to the fact that the stress wave propagation is sensitive to the transmission path, which in turn is affected significantly by the type and amount of grease present in the vicinity of the working elements of a bearing. Also, allowing SW signatures to travel over longer distances, after transmission across an interface, will result in a more pronounced effect on the signature shape.

To the author's knowledge, this particular technique has never been used before to determine the amount of grease present inside a low-speed rolling element bearing. The PIT method has been specially developed for bearings used in a RBC in which the end shaft is accessible. However, the PIT technique can also be applied to other slow rotating machinery provided that the end shaft is accessible and the shaft rotates at such a speed that would allow the transmitting transducer to be mounted onto the rotating shaft.

6.0 References

1 *SKF general catalogue* 1981, SKF, Sweden.

2 Vary, A. 1982, Acousto-ultrasonic charaterization of fiber reinforced composite, *Materials evaluation*, Vol 40, May 1982, pp 650-662.

3 William Jr., J.H. Kahn, E.B. and Lee, S.S. 1983, Effects of specimen resonance on acousto-ultrasonic testing. *Materials evaluation*, vol 41, no. 13, pp 1502-1510.

4 Kiernan, M.T. and Duke , J.C. Jr. 1988, PC analysis of an acousto-ultasonic signal, *Material evaluation*, vol 46, no.7, pp1105-1113.

5 Aduda, B.O. and Rawlings, R.D. 1996, Spectral analysis of acousto-ultrasonic waves for defect sizing. *NDT & E International*, Vol. 94, No. 4, pp 237-240.

6 Kwon, O.Y. and Lee, S.H 1999, Acousto-ultrasonic evaluation of adhesively bonded CFRP-aluminum joints, *NDT & E International*, Vol 32, no. 3, April 1999, pp153-160.

7 Mba, D., Bannister, R.H., and Findlay, G.E. 1999, Condition monitoring of low-speed rotating machinery using stress waves: Part I, *Proceedings of the Instn Mech Engrs,* Vol. 213, Part E, pp 153-170.

8 Mba, D., Bannister, R.H., and Findlay, G.E. 1999, Condition monitoring of low-speed rotating machinery using stress waves: Part II, *Proceedings of the Instn Mech Engrs,* pp 171-185, Vol. 213, Part E.

9 Heemskerk, R.S., Vermeiren, K.N. and Dolfsma, H. 1982, Measurement of lubrication condition in rolling element bearings, *ASLE Transactions*, vol 25, no 4, pp 519-527.

10 ESDU 1995, Film thicknesses in lubricated Hertzian contacts (EHL). Part 1: two-dimensional contacts (line contacts), Item no. 85027, *Engineering Sciences Data Unit*, London.

11 Hamrock, B.J. and Jacobson, B.B., 1984, Elastohydrodynamic lubrication of line contacts. *ASLE Transactions*, Vol 27, No 4, pp 275-287.

12 Chan, D.Y.C. and Horn, R.G. 1985, The drainage of thin liquid films between solid surfaces, *Journal of Chemical Physics*, Vol. 83, No. 10, pp5311-5324.

13 Chang, L., Cusano, C. and Conry, T.F. 1989, Effect of lubricant rheology and kinematic conditions on micro-elastohydrodynamic lubrication, Transaction of ASME *Journal of Tribology*, Vol 111, No. 2, pp 344-351.

14 Gee, M.L., McGuiggan, P.M. and Israelachvilli, J.C. 1990, Liquid to solidlike transitions of molecularly thin films under shear, *Journal of Chemical Physics*, Vol. 93, No. 3, pp 1895-1906.

15 Johnston, G.J., Wayte, R., and Spikes, H. 1991, The measurement and study of very thin lubricant films in concentrated contacts, *STLE Tribology Transactions*, Vol. 34, No. 2, pp 187-194.

16 Jang, S. and Tichy, J., 1995, Rheological models for thin film EHL contacts, Transaction of ASME, *Journal of Tribology*, Vol. 117, Jan 1995, pp 22-35.

17 Tichy, J.A. 1995, Modelling of thin film lubrication, *STLE Tribology Transactions*, Vol. 38, No. 1, Jan 1995, pp 108-118.

18 Luo, J., Wen, S. and Huang, P. 1996, Thin film lubrication, Part I: Study on the transition between EHL and thin film lubrication using a relative optical interference intensity technique, *Wear*, vol 194, pp 107-115.

19 Oksa, G. and Bahna, J. 1995 Matched predictive filter enhancement recognition of bursts. *Proceedings on the Symposium on Nuclear Reactor surveillance and diagnostics*. Session 10, Avignon, France.

20 Kay, S.M, and Marple, S.L Jr. 1981 Spectrum analysis - A modern perspective. *Proceedings of the IEEE,* pp 1380-1419, Vol. 69, No. 11.

21 Makhoul, J. 1975 Linear prediction: A tutorial review. *In Proc. Of the IEEE,* PP 561-580, Vol. 63, No. 4.

22 Haykin, S. 1984 *Introduction to adaptive filters*. Macmillan Publishing Company, New York. ISBN 0 - 02 - 949460 - 5.

23 Everitt, B. 1974 *Cluster analysis*. Published on behalf of the Social Science Research Council by Heinemann Educational Books New York: Halsted Press. ISBN 0 435 82297 7.